Geotextiles and Geomembranes xxx (2015) 1–6

Contents lists available at ScienceDirect

Geotextiles and Geomembranes

journal homepage: www.elsevier.com/locate/geotexmem

Technical note

Numerical study on ground improvement for liquefaction mitigation using stone columns encased with geosynthetics

Liang Tang [a, b, *], Shengyi Cong [a, b], Xianzhang Ling [a, **], Jinchi Lu [c], Ahmed Elgamal [c]

[a] School of Civil Engineering, Harbin Institute of Technology, Harbin, Heilongjiang 150090, China
[b] State Key Laboratory of Geological Disaster Prevention and Geological Environment Protection, Chengdu University of Technology, Chengdu, Sichuan 610059, China
[c] Department of Structural Engineering, University of California, San Diego, 9500 Gilman Drive, La Jolla, CA 92093, United States

A R T I C L E I N F O

Article history:
Received 3 June 2014
Received in revised form
24 November 2014
Accepted 27 November 2014
Available online xxx

Keywords:
Soil liquefaction
Stone column
Geosynthetic encasement
Remediation
Finite element analysis
Earthquake

A B S T R A C T

The geosynthetic-encased stone column (ESC) strategy has been extensively used for improving soft soils. However, no studies have been conducted to assess the use of ESCs to mitigate sand strata. In this study, three-dimensional finite element (FE) analyses were conducted to explore the mitigation of mildly sloped saturated sand strata using ESC approaches. We investigated the encasement effect in ESC remediation and the effect of the following important design parameters in reducing lateral ground deformation: the thickness, the tensile stiffness, and the permeability of the geosynthetic; the ESC diameter; and the distributed load at the stone column (SC) surface. The results showed that the ESC remediation reduced more lateral deformation, compared to the SC approach. The ground stiffening was also dramatically enhanced as the stiffness and thickness of the geosynthetic and the ESC diameter were increased, but the encased efficiency gradually decreased. The lateral ground displacement began to decrease significantly when the permeability of the geosynthetic exceeded 0.1 m/s. The larger surface load did not prevent soil liquefaction, but it produced significantly less displacements and virtually no permanent deformation.

1. Introduction

The liquefaction-induced lateral spreading of mildly sloping ground during earthquakes can cause major destruction to foundations and associated buildings (Fiegel and Kutter, 1994; Kishida, 1966). Several methods, such as gravel drains/stone columns (SCs), densification, and solidification, are available to reduce the liquefaction risk and the associated ground deformation (Adalier et al., 2003; Baez, 1995; Gniel and Bouazza, 2009; Lo et al., 2010; Shen et al., 2005). Among these methods, the SC technique is preferred for mitigating liquefaction hazards because of its effectiveness and the simple construction involved (Adalier et al., 2003). A novel SC technique has recently been developed in which an individual SC is encased by a geosynthetic layer and does not involve an encasement, unlike the traditional SC approach (Sharma et al., 2004).

The ESC technology has proven to be an economical ground improvement technique for soft soils and has been effectively used to reduce the deformation of soft foundations (Sharma et al., 2004). Many researchers have conducted numerical analyses and experimental studies on the behavior of soft ground that has been improved using ESCs (Katti et al., 1993; Murugesan and Rajagopal, 2009).

Extensive research has been carried out on various applications of ordinary SCs without encasement and to assess the effectiveness of these methods for liquefaction mitigation using field case histories (Miwa et al., 2006; Saxena and Hussin, 1997), field tests (Ashford et al., 2006), physical experiments (Adalier et al., 2003; Ali et al., 2014; Dash and Bora, 2013; Haldar and Babu, 2010; Murugesan and Rajagopal, 2009; Najjar et al., 2010; Wilson et al., 2000), and numerical simulation (Almeida et al., 2013; Castro and Karstunen, 2010; Elgamal et al., 2009; Khabbazian et al., 2010; Lu et al., 2011; Murugesan and Rajagopal, 2006; Yoo, 2010).

* Corresponding author. School of Civil Engineering, Harbin Institute of Technology, Harbin, Heilongjiang 150090, China. Tel.: +86 (0) 451 86282095; fax: +86 (0) 451 86282704.
** Corresponding author.
E-mail address: hit_tl@163.com (L. Tang).

http://dx.doi.org/10.1016/j.geotexmem.2014.11.011
0266-1144/

Please cite this article in press as: Tang, L., et al., Numerical study on ground improvement for liquefaction mitigation using stone columns encased with geosynthetics, Geotextiles and Geomembranes (2015), http://dx.doi.org/10.1016/j.geotexmem.2014.11.011

Recently, Elgamal et al. (2009) conducted three-dimensional (3D) FE simulations using the open-source computational platform OpenSees (http://opensees.berkeley.edu, Mazzoni et al., 2006) with the aid of OpenSeesPL as a pre- and post-processing tool (Lu, 2006) and evaluated the liquefaction mitigation of sand strata via then SC approach. Later, Asgari et al. (2013) assessed the effectiveness of the SC method for a liquefiable stratum based on several important factors using OpenSeesPL. Rayamajhi et al. (2014) systematically studied the shear stress distribution for discrete columns in liquefiable soils using OpenSeesPL. However, no studies have been conducted on the liquefaction mitigation of sand strata that have been improved by ESCs.

In this study, we use FE simulations to investigate the effectiveness of remediation using the ESC technique for sand strata. The results of this parametric study are used to highlight the effect of important parameters on the lateral extent of remediation. Finally, insights and conclusions are drawn based on the reported results.

2. Numerical modeling

2.1. Computational formulation

The open-source computational platform OpenSees (Mazzoni et al., 2006) was used to perform all of the FE simulations, which are efficiently executed using OpenSeesPL (Lu, 2006).

The 3D FE modeling of the soil and the SC was carried out using the 20-8 noded, effective-stress solid–fluid fully coupled brick element (Lu, 2006). This element is based on the solid–fluid formulation for saturated soil. A total of 20 nodes are used to describe the solid translational degrees of freedom, and 8-corner nodes are used to represent the fluid pressure (Chan, 1988; Yang, 2000). The SC and the soil were modeled using a multi-surface-plasticity constitutive model (Yang, 2000; Yang et al., 2003).

The geosynthetic encasement around the SC was modeled as a linear elastic material for simplicity (Ghazavi and Nazari, 2013; Han and Gabr, 2002; Keykhosropur et al., 2012; Lo et al., 2010; Murugesan and Rajagopal, 2006; Pulko et al., 2011; Wu and Hong, 2014; Yoo, 2010). The value of E for the geosynthetic was derived from the relationship $J = E \times t$, where t is the thickness of the element representing the geosynthetic, and J is the tensile stiffness of the geosynthetic, which is defined as the ratio of the tensile force per unit width to the average strain. The geosynthetic was discretized into 20-node brick solid elements. The mass density of the geosynthetic was 1500 kg/m^3 (Giroud, 1994) and its Poisson ratio was 0.3 (Murugesan and Rajagopal, 2006), respectively.

2.2. Model cases for SC and ESC

Typical SCs [Fig. 1(a)] were constructed in a grid pattern to improve the sand stratum covering the entire building footprint. A "unit cell" (i.e., a representative area of improved soil) with a Periodic boundary was used to model the remediated area with a large spatial extent. Using this approach, a half-mesh for a representative cell was explored using the following boundary conditions: (1) the penalty method was used to set equal displacement degrees of freedom for the corresponding left and right boundary nodes at any spatial location in the horizontal and vertical directions (Periodic boundary); (2) the inner (symmetric) and outer boundaries were fixed against out-of-plane displacement but are free to move longitudinally and vertically; (3) the soil surface was stress-free; (4) the seismic excitation was imposed on the base along the x-axis, and a scaled El Centro (1940) north–south acceleration record (Chopra, 2001) with a peak value of 0.2 g was applied (Fig. 2).

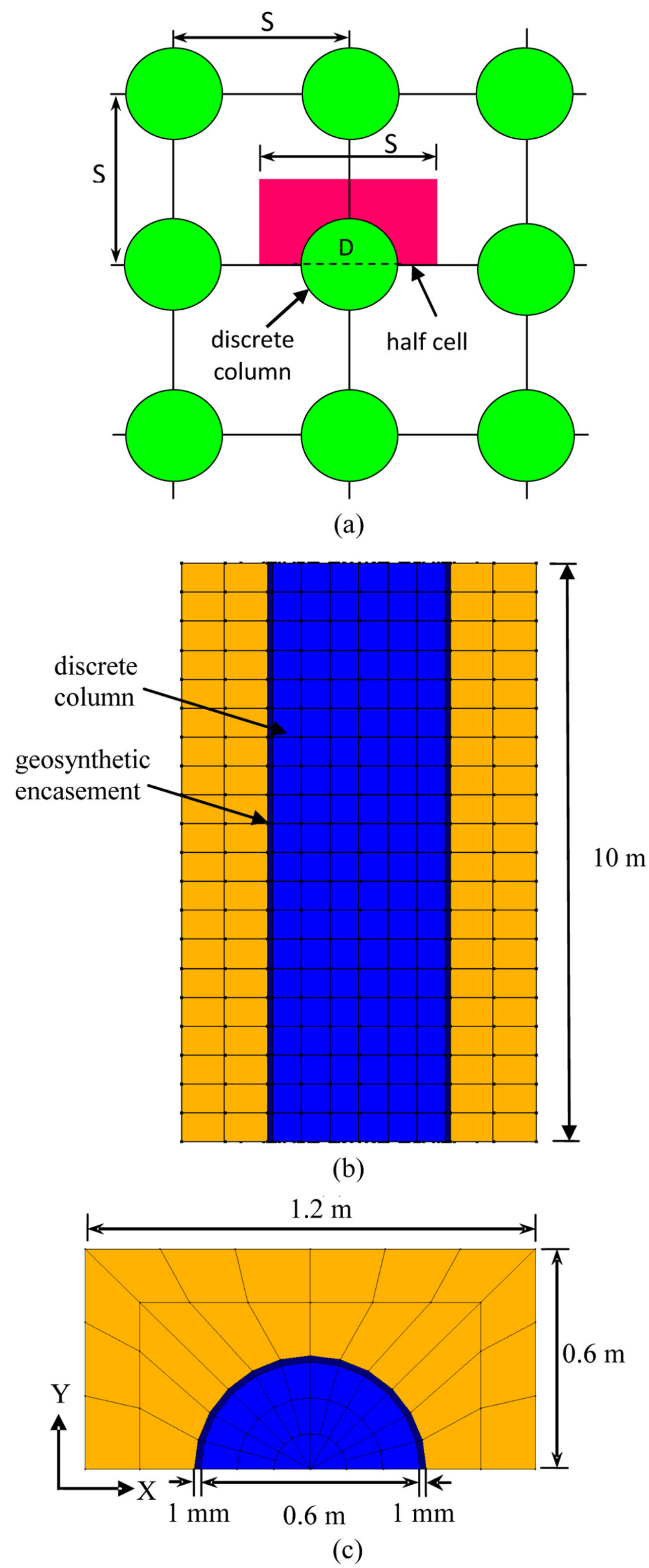

Fig. 1. FE mesh for ground modification by geosynthetic-reinforced SC (dark zone represents remediated domain; replacement ratio $A_r = 20\%$; SC diameter $D = 0.6$ m): (a) Schematic plan view of discrete column layout; (b) FE model elevation (1/2 mesh used because of symmetry); and (c) plan view (3D mesh).

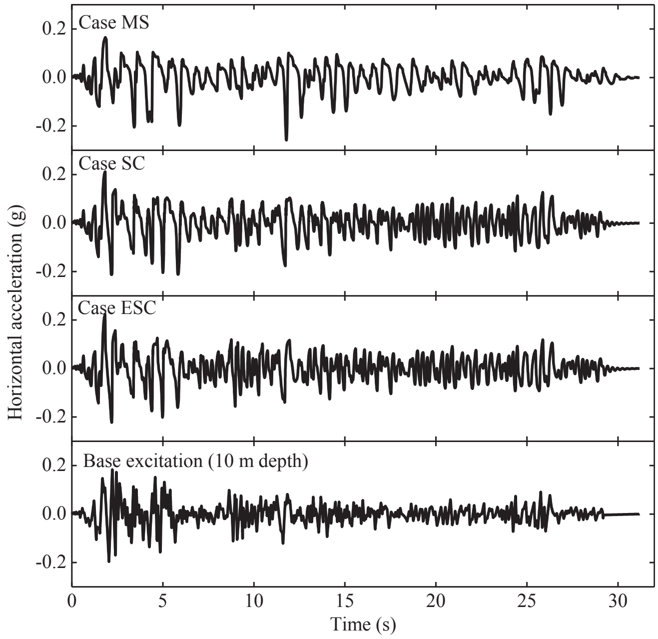

Fig. 2. Horizontal ground surface accelerations for Cases MS, SC, and ESC.

A 10-m-thick saturated Nevada sand layer at a Relative Density of approximately 40%, with an inclination of 4° (the model was inclined), was used in all the simulations, and the material properties are given in Table 1, as reported in Elgamal et al. (2009).

Remediation by SC and ESC treatment was investigated to reduce the liquefaction-induced lateral deformation. The area replacement ratio A_r is conventionally defined as the ratio of the SC area A_{sc} to the tributary area A (i.e., $A_r = A_{sc}/A = \pi D^2/4S^2$), where D = SC diameter and S = distance (spacing) between the SC centers [Fig. 1(a)]. For all the SC and ESC cases, the diameter and the length of the SC were maintained at 0.6 m and 10 m, respectively. A column extends throughout the full soil layer [Fig. 1(b)]. The A_r was set as to 20%, and the center-to-center spacing 'S' between the SCs is 1.2 m.

For simplicity, the interface between the geosynthetics [Fig. 1(c)] and the soil was assumed to be fully bonded in the study. The geosynthetic with a high permeability of 1.0 m/s was selected, and 2% Raleigh damping is used for both the improved and unimproved cases (Rayamajhi et al., 2014).

Based on the above parameters, the SC and ESC were employed to improve the performance of the sand stratum using the benchmark models as Cases SC and ESC, where the t and J values for the geosynthetic were defined as 0.001 m and 1000 kN/m, respectively. The medium sand case (Case MS) represents the benchmark of the original unremediated situation at a Medium relative density. The results of Case MS results serve as a reference for the free-field response.

Table 1
Soil model parameters (Elgamal et al., 2009).

Parameters	Medium sand	Dense sand (SCs)
Mass density (kg/m^3)	1900	2100
Low-strain shear modulus (at 80 kPa mean effective confinement, MPa)	78.5	135.0
Friction angle	31.4°	40.0°
Liquefaction yield strain	0.01	0
Contraction parameter	0.3	0.1
Phase transformation angle	26.5°	26.0°
Dilation parameter (d_1)	0.4	0.8
Dilation parameter (d_2)	2.0	5.0
Permeability (m/s)	6.6e−005	1.0e−007

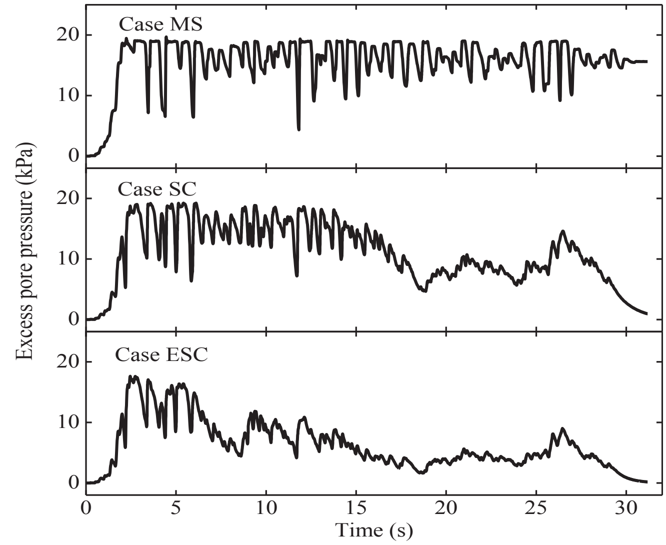

Fig. 3. Excess pore pressure time histories along FE mesh center at 2-m depth for Cases MS, SC, and ESC (with effective vertical stress = 19.4 kPa).

3. Response characteristics of benchmark cases

The excess pore pressure (u_e) at 2-m depth for Case MS reaches a peak and subsequently attains a nearly constant high level up to the end of shaking at 31.18 s (Fig. 3): full liquefaction simultaneously appears at this depth. However, the u_e in Case SC decreases to a lower value after approximately 13.5 s despite reaching the same high level as in Case MS. In Case ESC, the u_e increases somewhat more slowly, reaching a slightly lower ultimate value, and dissipation occurs faster than in Case SC. Thus, the SC and ESC do not appear to preclude significant u_e generation (Fig. 3).

In Case MS, acceleration spikes appearing exclusively in the negative direction (Fig. 2) shows that the mild 4° inclination imposes a static driving shear stress component (due to gravity),

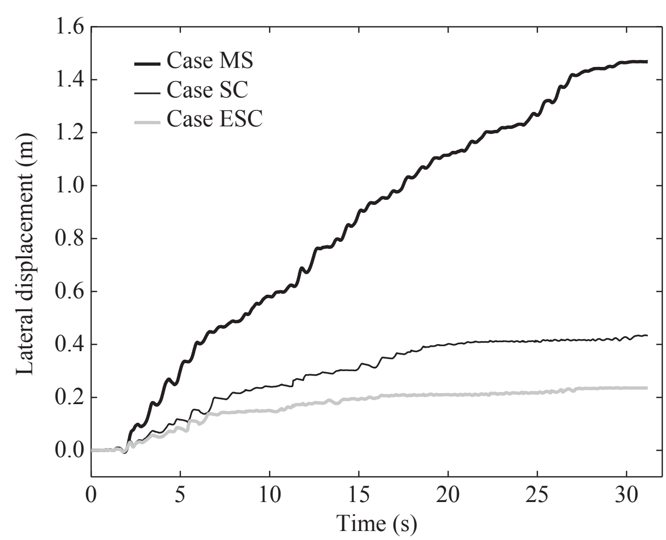

Fig. 4. Lateral ground surface displacement along FE mesh center for Cases MS, SC, and ESC.

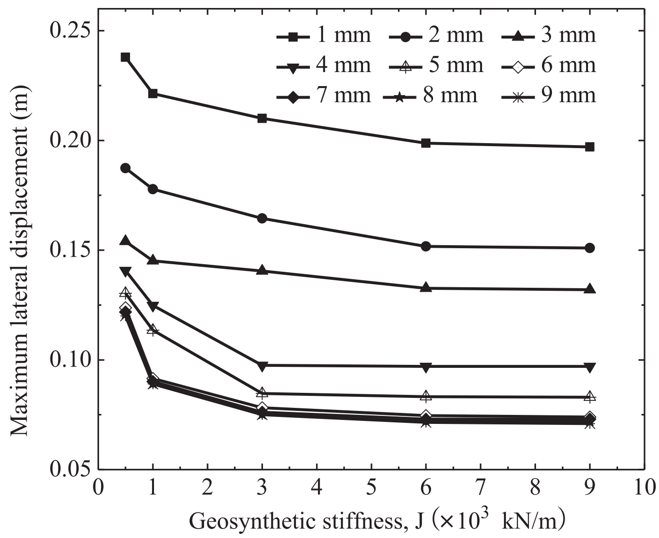

Fig. 5. Effect of geosynthetic stiffness on maximum lateral surface displacements along FE mesh center.

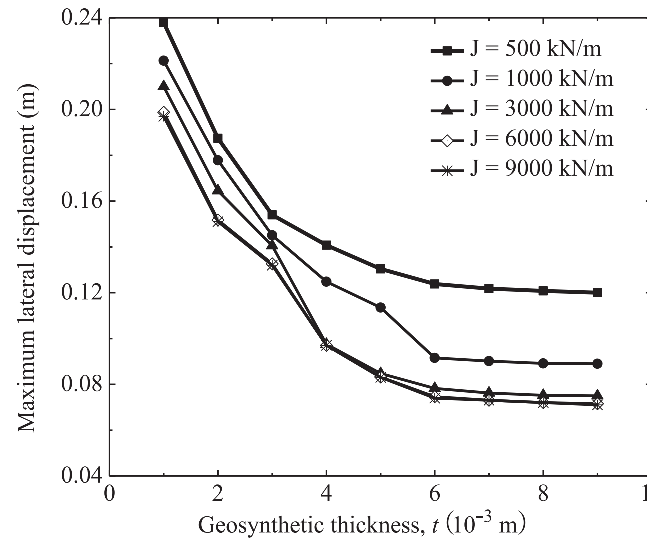

Fig. 6. Effect of geosynthetic thickness on maximum lateral surface displacements along FE mesh center.

causing a significantly accumulated downslope deformation at the ground surface with high levels of 1.47 m (Fig. 4) during the strong shaking phase.

The lateral ground surface deformation for Cases SC and ESC (Fig. 4) is overall lower than that of Case MS, and no asymmetric pattern can be observed in the acceleration time histories (Fig. 2). Although the sand stratum is improved using SC and ESC, the u_e remained almost the same, and the encasement of SCs clearly played an appreciably beneficial role in reducing the ground surface deformation. Thus, encasing the ESC with a geosynthetic can increase the stiffness of the foundation.

4. Results and discussion

The remediation of a sand stratum using SC and ESC techniques was explored through a parametric study based on Case ESC. The reduction of the accumulated lateral deformation serves as an indicator of the remediation efficacy.

4.1. Influence of encasement stiffness and thickness

Figs. 5 and 6 show the influence of the J and t values, respectively, of the geosynthetic on the maximum lateral ground surface displacements at the SC center. The displacements (Fig. 5) gradually decrease because of the increasing J in the wide range from 1000 kN/m to 9000 kN/m (Ingold and Miyata, 1996). Similarly, the displacements (Fig. 6) also decrease significantly because of the increased t value. Furthermore, the ultimate deformation approaches a constant value for a specific thickness in the range of 0.001–0.009 m as J exceeds 6000 kN/m. This tendency agrees with the observation that almost no reduction of lateral deformation is observed when t exceeds 0.006 m.

Thus, increasing the J and t of the geosynthetic could significantly reduce the lateral ground surface deformation; however, the reduction in of lateral deformation becomes negligible if J or t continues to increase to a critical value. Moreover, the remediation efficacy of the ESCs is significantly reduced as t and J increase, and consequently, the ultimate ground surface deformation can be reduced to approximately 0.071 m simply by increasing the J and t of the geosynthetic.

4.2. Effect of geosynthetic permeability

A geosynthetic, i.e., a planar product that is manufactured from a polymeric material, is used together with geotechnical-related materials. Geosynthetics are often categorized into four basic groups: geotextiles, geo-grids, geo-membranes, and geo-composites. Accordingly, different permeability values are associated with each of these basic groups. The effect of the geosynthetic permeability on lateral ground deformation was investigated by varying the permeabilities over the range of 1×10^{-4} m/s to 20 m/s using Case ESC.

A slight reduction in the ground deformation is observed when the permeability is below 0.01 m/s (Fig. 7), indicating that there is no apparent stiffening effect from the encasement. Indeed, the deformation is significantly reduced when the permeability exceeds 0.1 m/s (Fig. 7). The figure shows that the increased

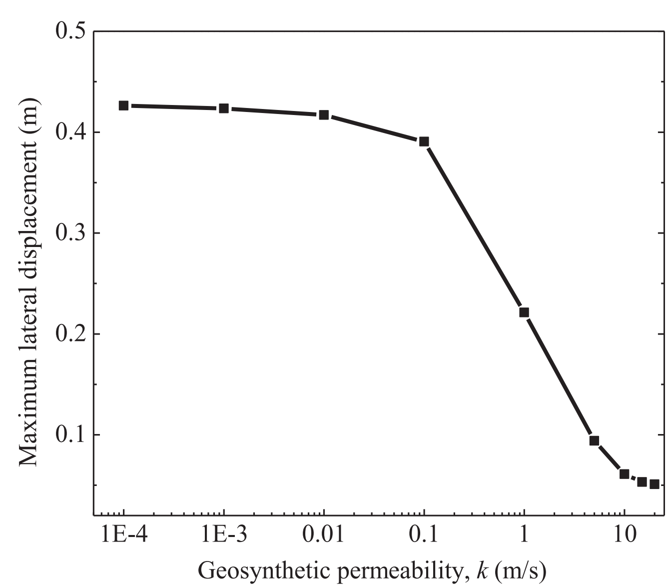

Fig. 7. Effect of geosynthetic permeability on maximum lateral surface displacements along FE mesh center.

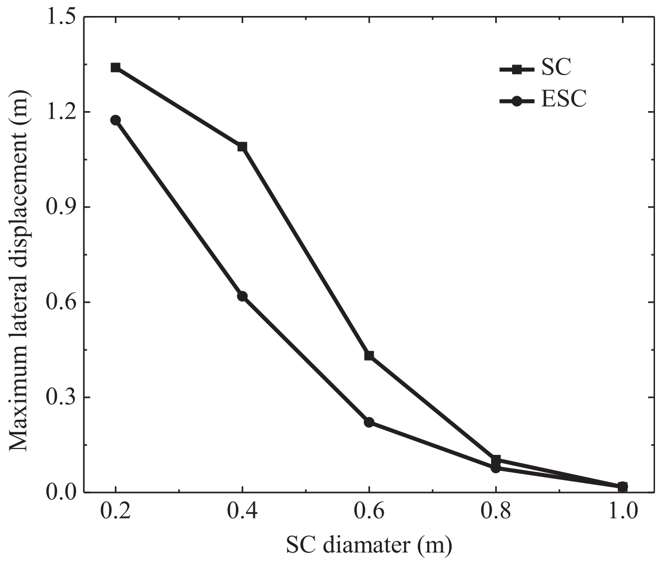

Fig. 8. Effect of SC diameter on maximum surface displacement along FE mesh center.

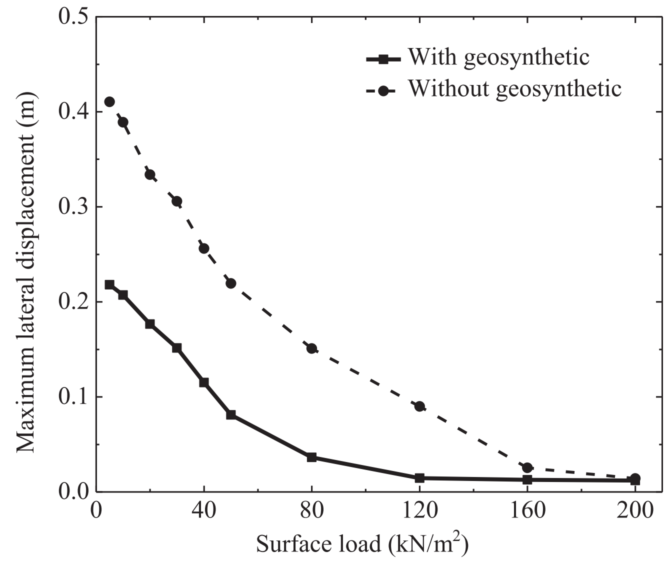

Fig. 9. Effect of surface load on maximum lateral surface displacement along FE mesh center.

foundation stiffness from the ESCs does not appear during shaking for a small permeability. This result indicates that a sufficiently large permeability is required for the geosynthetic such that water can pass freely from the soil through the fabric to quickly dissipate the high u_e that has been generated.

4.3. Effect of SC diameter

Fig. 8 shows the effect varying the SC diameter on the maximum surface displacement at the center of the SC for Cases SC and ESC. For ground reinforcement using SCs and ESCs, all the ground surface displacements are significantly diminished when the diameter increases from 0.2 m (i.e., $A_r = 2\%$) to 1.0 m (i.e., $A_r = 55\%$). A larger diameter results in a lower lateral accumulated deformation, which essentially produces a greater mobilized soil wedge at the front of the SC that effectively resist the load from the moving soil at the downslope. Thus, the ground deformation is restrained prior to the yielding of the remediated zone.

Furthermore, the difference in the reduction in the lateral deformation between the SC and ESC strategies gradually decreases as the diameter increases. Specifically, the ultimate deformation reaches approximately 0.018 m as the diameters of SC and ESC approach 1.0 m, with virtually no appreciable beneficial effects induced by encasement by the geosynthetic.

The lateral deformation can be reduced to a tolerable level for the design of a structure that is located on the sand stratum if the SCs have a sufficiently large diameter. However, an excessively large diameter (i.e., a high A_r) may be prohibitively expensive and impractical to implement (e.g., an A_r above 20%). Therefore, installed ESCs are a potential solution for improving the sand stratum.

4.4. Influence of surface load at the SC zone

In general, the lateral surface deformation (which is also shown by the displacement data) drastically decreases regardless of SC and ESC remediation when the load is gradually increased (Fig. 9). The displacements of the foundations improved with SCs and ESCs are reduced by approximately 98% (from 0.43 m without a load to 0.01 m with a load of 200 kPa) and approximately 96% (from 0.24 m without a load to 0.01 m with a load of 200 kPa), respectively. Moreover, the ultimate deformation based on Case ESC reaches a low level once the load approaches 120 kPa, whereas a load greater than 160 kPa can cause a substantially lower final deformation using SCs. Note that the lateral deformations for the ESC and SC cases are nearly identical when the load reaches 200 kPa.

These observations suggest that a sufficient vertical stress, i.e., greater than approximately 160 kPa in the SC cases and approximately 120 kPa in the ESC cases, may be required to produce a beneficial reduction in the ground deformation to a low or nearly zero level because using an SC and an ESC with the load significantly promoted the overall foundation stiffness. In practice, confinement could be achieved using the weight of the structure.

5. Summary and conclusions

A study was conducted using a nonlinear FE analysis to explore the effect of SCs and ESCs on liquefaction-induced lateral deformation. The objective of the study was to investigate the effectiveness of SC and ESC mitigation approaches by varying several key design parameters to achieve satisfactory, low levels of permanent deformation. The primary findings from this study are summarized below.

(1) In general, both SC and ESC remediation were found to be effective in reducing the sand stratum lateral deformation. Overall, the ESCs produced a stiffer ground reinforcement, which generated less lateral ground displacements than using SC mitigation because of full encasement by the geosynthetic and amplified the seismic waves on the ground surface and the upper stratum.
(2) For a special sand stratum, using a geosynthetic with larger t and J values was found to significantly decrease the lateral ground deformation, where the threshold values for t and J to achieve remediation were 6×10^3 kN/m and 6×10^{-3} kN/m, respectively.
(3) A geosynthetic with permeability less than 0.1 m/s was observed to be insensitive to permanent deformation. In addition, increasing the permeability above 1.0 m/s decreased the lateral deformation.

Please cite this article in press as: Tang, L., et al., Numerical study on ground improvement for liquefaction mitigation using stone columns encased with geosynthetics, Geotextiles and Geomembranes (2015), http://dx.doi.org/10.1016/j.geotexmem.2014.11.011

(4) For the SC and ESC cases, increasing the SC diameter effectively reduced the lateral deformation of the sand strata, even when there was virtually no lateral deformation, if the diameter reached 1.0 m. However, the use of an SC with an appropriate replacement ratio as low as 20% did not result in satisfactory outcomes, and ESC mitigation generated tolerable lower lateral deformations.
(5) The stiffening benefit due to the larger load applied at the SC zone produced significantly less lateral displacement or virtually no permanent deformation when the load approached 120 kPa for the ESC cases and 160 kPa for the SC cases.
(6) Additional experimental data are needed to further explore the complex patterns of ESC strategies, particularly for the cases of: (i) stratified soil profiles, (ii) looser or denser soil formations, (iii) different thicknesses of treated deposits, (iv) ESC length and spacing, (v) initial column stiffness, and (vii) more realistic seismic ground excitation.

Acknowledgments

We gratefully acknowledge support for this research from the National Natural Science Foundation of China (Grant No. 51108134 and 51378161), and the Applied Technology Research and Development Plan Program of Heilongjiang Province, China (No. GZ13A009).

References

Adalier, K., Elgamal, A., Meneses, J., Baez, J., 2003. Stone columns as liquefaction countermeasure in non-plastic silty soils. Soil Dyn. Earthq. Eng. 23 (7), 571–584.

Ali, K., Shahu, J.T., Sharma, K.G., 2014. Model tests on single and groups of stone columns with different geosynthetic reinforcement arrangement. Geosynth. Int. 21 (2), 103–118.

Almeida, M.S.S., Hosseinpour, I., Riccio, M., 2013. Performance of a geosynthetic-encased column (GEC) in soft ground: numerical and analytical studies. Geosynth. Int. 20 (4), 252–262.

Asgari, A., Oliaei, M., Bagheri, M., 2013. Numerical simulation of improvement of a liquefiable soil layer using stone column and pile-pinning techniques. Soil Dyn. Earthq. Eng. 51, 77–96.

Ashford, S.A., Juirnarongrit, T., Sugano, T., Hamada, M., 2006. Soil-pile response to blast-induced lateral spreading. I: field test. J. Geotech. Geoenviron. Eng. 132 (2), 152–162.

Baez, J.I., 1995. A Design Model for the Reduction of Soil Liquefaction by Using Vibro-stone Columns (Ph.D. thesis). University of Southern California, Los Angeles.

Castro, J., Karstunen, M., 2010. Numerical simulations of stone column installation. Can. Geotech. J. 47 (10), 1127–1138.

Chan, A.H.C., 1988. A Unified Finite Element Solution to Static and Dynamic Problems in Geomechanics (Ph.D. thesis). Swansea University, U.K.

Chopra, A.K., 2001. Dynamics of Structures: Theory and Applications to Earthquake Engineering, second ed. Prentice Hall, New Jersey.

Dash, S.K., Bora, M.C., 2013. Influence of geosynthetic encasement on the performance of stone columns floating in soft clay. Can. Geotech. J. 50 (7), 754–765.

Elgamal, A., Lu, J., Forcellini, D., 2009. Mitigation of liquefaction-induced lateral deformation in a sloping stratum: three-dimensional numerical simulation. J. Geotech. Geoenviron. Eng. 135 (11), 1672–1682.

Fiegel, G.L., Kutter, B.L., 1994. Liquefaction-induced lateral spreading of mildly sloping ground. J. Geotech. Eng. 120 (12), 2236–2243.

Ghazavi, M., Nazari, A.J., 2013. Bearing capacity of geosynthetic encased stone columns. Geotext. Geomembr. 38, 26–36.

Giroud, J.P., 1994. Relationship between geomembrane density and carbon black content. Geosynth. Int. 1 (1), 93–98.

Gniel, J., Bouazza, A., 2009. Improvement of soft soils using geogrid encased stone columns. Geotext. Geomembr. 27 (3), 167–175.

Haldar, S., Babu, G.L.S., 2010. Failure mechanisms of pile foundations in liquefiable soil: parametric study. Int. J. Geomech. 10 (2), 74–84.

Han, J., Gabr, M.A., 2002. Numerical analysis of geosynthetic-reinforced and pile-supported earth platforms over soft soil. J. Geotech. Geoenviron. Eng. 128 (1), 44–53.

Ingold, T.S., Miyata, K., 1996. Walls reinforced with fiber reinforced plastic geogrids in Japan. Geosynth. Int. 3 (1), 1–11.

Katti, R.K., Katti, A.R., Naik, S., 1993. Monograph to Analysis of Stone Columns with and without Geosynthetic Encasement. CBIP Publication, New Delhi.

Keykhosropur, L., Soroush, A., Imam, R., 2012. 3D numerical analyses of geosynthetic encased stone columns. Geotext. Geomembr. 35, 61–68.

Khabbazian, M., Kaliakin, V.N., Meehan, C.L., 2010. Numerical study of the effect of geosynthetic encasement on the behaviour of granular columns. Geosynth. Int. 17 (3), 132–143.

Kishida, H., 1966. Damage to reinforced concrete buildings in Niigata city with special reference to foundation engineering. Soils Found. 6 (1), 71–88.

Lo, S.R., Zhang, R., Mak, J., 2010. Geosynthetic-encased stone columns in soft clay: a numerical study. Geotext. Geomembr. 28 (3), 292–302.

Lu, J., 2006. Parallel Finite Element Modeling of Earthquake Site Response and Liquefaction (Ph.D. thesis). University of California, San Diego.

Lu, J., Elgamal, A., Yan, L., Law, K.H., Conte, J.P., 2011. Large scale numerical modeling in geotechnical earthquake engineering. Int. J. Geomech. 11 (6), 490–503.

Mazzoni, S., McKenna, F., Scott, M.H., Fenves, G.L., 2006. Open System for Earthquake Engineering Simulation User Manual. University of California, Berkeley, California. http://opensees.berkeley.edu/.

Miwa, S., Ikeda, T., Sato, T., 2006. Damage process of pile foundation in liquefied ground during strong ground motion. Soil Dyn. Earthq. Eng. 26 (2), 325–336.

Murugesan, S., Rajagopal, K., 2006. Geosynthetic-encased stone columns: numerical evaluation. Geotext. Geomembr. 24 (6), 349–358.

Murugesan, S., Rajagopal, K., 2009. Studies on the behavior of single and group of geosynthetic encased stone columns. J. Geotech. Geoenviron. Eng. 136 (1), 129–139.

Najjar, S.S., Sadek, S., Maakaroun, T., 2010. Effect of sand columns on the undrained load response of soft clays. J. Geotech. Geoenviron. Eng. 136 (9), 1263–1277.

Pulko, B., Majes, B., Logar, J., 2011. Geosynthetic-encased stone columns: analytical calculation model. Geotext. Geomembr. 29 (1), 29–39.

Rayamajhi, D., Nguyen, T., Ashford, S., Boulanger, R., Lu, J., Elgamal, A., Shao, L., 2014. Numerical study of shear stress distribution for discrete columns in liquefiable soils. J. Geotech. Geoenviron. Eng. 140 (3), 04013034.

Saxena, D.S., Hussin, J.D., 1997. Stone column improved and piezocone tested site supports mid rise building complex – a case history. In: Geotech. Spec. Publ., vol. 69. ASCE, pp. 476–491.

Sharma, S.R., Phanikumar, B.R., Nagendra, G., 2004. Compressive load response of granular piles reinforced with geogrids. Can. Geotech. J. 41 (1), 187–192.

Shen, S.L., Chai, J.C., Hong, Z.S., Cai, F.X., 2005. Analysis of field performance of embankments on soft clay deposit with and without PVD-improvement. Geotext. Geomembr. 23 (6), 463–485.

Wilson, D.W., Boulanger, R.W., Kutter, B.L., 2000. Observed seismic lateral resistance of liquefying sand. J. Geotech. Geoenviron. Eng. 126 (10), 898–906.

Wu, C.S., Hong, Y.S., 2014. A simplified approach for evaluating the bearing performance of encased granular columns. Geotext. Geomembr. 42 (4), 339–347.

Yang, Z., 2000. Numerical Modeling of Earthquake Site Response Including Dilation and Liquefaction (Ph.D. thesis). Columbia University, New York.

Yang, Z., Elgamal, A., Parra, E., 2003. Computational model for cyclic mobility and associated shear deformation. J. Geotech. Geoenviron. Eng. 129 (12), 1119–1127.

Yoo, C., 2010. Performance of geosynthetic-encased stone columns in embankment construction: numerical investigation. J. Geotech. Geoenviron. Eng. 136 (8), 1148–1160.